Human Molecular Genetics, 2017, Vol. 26, No. 21 4203–4214

doi: 10.1093/hmg/ddx310
Advance Access Publication Date: 13 August 2017
Original Article

ORIGINAL ARTICLE

Abnormal creatine transport of mutations in monocarboxylate transporter 12 (MCT12) found in patients with age-related cataract can be partially rescued by exogenous chaperone CD147

Andrina Stäubli[1,2,†], Nadejda Capatina[1,†], Yvonne Fuhrer[1,†], Francis L. Munier[3], Stephan Labs[1], Daniel F. Schorderet[4,5], Amit Tiwari[1], Francois Verrey[6,7], Elise Heon[8], Ching-Yu Cheng[9,10,11], Tien-Yin Wong[9,10,11], Wolfgang Berger[1,7,12], Simone M.R. Camargo[6,7] and Barbara Kloeckener-Gruissem[1,2,*]

[1]Institute of Medical Molecular Genetics, University Zurich, Zurich, Switzerland, [2]Department of Biology, ETH, Zurich, Switzerland, [3]Jules-Gonin Eye Hospital, University Lausanne, Lausanne, Switzerland, [4]Faculty of Life Sciences, Ecole Polytechnique Fédérale de Lausanne, Institute for Research in Ophthalmology, Sion, Lausanne, Switzerland, [5]Department of Ophthalmology, University of Lausanne, Lausanne, Switzerland, [6]Institute of Physiology and [7]Zurich Center for Integrative Human Physiology (ZIHP), University of Zurich, Zurich, Switzerland, [8]Department of Ophthalmology and Vision Sciences, Hospital for Sick Children, Toronto, Canada, [9]Singapore National Eye Centre, Singapore Eye Research Institute, Singapore, Singapore, [10]Ophthalmology & Visual Sciences Academic Clinical Program (Eye ACP), Duke-NUS Medical School, Singapore, Singapore, [11]Department of Ophthalmology, Yong Loo Lin School of Medicine, National University of Singapore, Singapore, Singapore and [12]Neuroscience Center Zurich (ZNZ), University and ETH Zurich, Zurich, Switzerland

*To whom correspondence should be addressed at: Institute of Medical Molecular Genetics, University Zurich, Wagistrasse 12, 8952 Schlieren, Switzerland. Tel: +41445563350; Fax: +41445563351; Email: kloeckener@medmolgen.uzh.ch

Abstract

Membrane transporters influence biological functions in the ocular lens. Here, we investigate the monocarboxylate transporter 12 (MCT12), also called creatine transporter 2 (CRT2), which is found in the ocular lens and is involved in cataract. As the age-related form affects about half of the population world-wide, understanding relevant pathomechanisms is a prerequisite for exploring non-invasive treatments. We screened the coding exons of the gene *SLC16A12* in 877 patients from five cohorts, including Caucasian and Asian ethnicities. A previously identified risk factor, SNP rs3740030, displayed different frequencies in the Asian cohorts but risk could not be established. In 15 patients 13 very rare heterozygous nucleotide substitutions were identified, of which eight led to non-synonymous and four to synonymous amino acid exchanges and one

[†]These authors contributed equally.

Received: June 6, 2017. **Revised:** July 11, 2017. **Accepted:** July 28, 2017

mapped to the canonical splice site in intron 3. Their impact on creatine transport was tested in *Xenopus laevis* oocytes and human HEK293T cells. Four variants (p.Ser158Pro, p.Gly205Val, p.Pro395Gln and p.Ser453Arg) displayed severe reduction in both model systems, indicating conserved function. Two of these, p.Gly205Val, and p.Ser453Arg, did not localize to the oocyte membrane, suggesting possible impacts on protein interactions for transporter processing. In support, exogenously supplied excess of MCT12's chaperone CD147 in HEK293T cells led to a partial recovery of the defective uptake activity from p.Gly205Val and also from mutant p.Pro395Gln, which did localize to the membrane. Our findings provide first insight in the molecular requirements of creatine transporter, with particular emphasis on rescuing effects by its chaperone CD147, which can provide useful pharmacological information for substrate delivery.

Introduction

Cataract is a condition of opacities within the ocular lens leading to visual deficits and eventually complete blindness. Based on age of onset, one can distinguish between juvenile (congenital or childhood) cataracts and the very common age-related cataracts (ARC). The juvenile form represents a small fraction of all cataracts and often exhibits Mendelian inheritance with over 30 involved genes (1–3). In contrast, the age-related form is considered a multifactorial disease where environmental and genetic factors influence the development of the disease. Despite its very high frequency of occurrence worldwide irrespective of ethnicity and economic conditions, only few genetic factors for ARC have been identified so far, primarily by genetic association studies. Among them are the structural protein crystalline alpha (*CRYAA*) (4), the glutathione S transferase (*GST*) (5,6), DNA repair enzymes *XRCC1*, *XPD* and *APE1* (7–9), the epithelial cell receptor protein tyrosine kinase (*EPHA2*) (10–12), and the monocarboxylate transporter MCT12 (creatine transporter CRT2) (*SLC16A12*) (13,14).

To supply the avascular lens with metabolites, membrane transporters are needed. One such transporter is MCT12 (OMIN 611910), which is 1 of 14 members of the *SLC16* monocarboxylate transporter family (15). Initially, it was shown to be associated with cataract by the finding of a premature stop codon mutation, which segregated in a large family with a syndromal autosomal dominant juvenile cataract (16). Consequently, mutations in *SLC16A12* were also found to associate with age-related cataract (13,14). Like other members of the MCT family, MCT12 translocates to the plasma membrane by interacting with the molecular chaperone CD147 (basigin), encoded by *BSG* (OMIM 109480) (17–20). CD147 is a ubiquitously expressed glycoprotein involved in many cellular functions, such as matrix metalloproteinase induction, inflammation and tumor invasion (21–25). The interaction between the chaperone and its MCT partners was shown to be important for the maturation process of both, CD147 and monocarboxylate transporters (26). Additionally, it is suggested that, once at the membrane, CD147 and MCTs stay together in oligoheterodimers to perform their task of substrate transport (19,20). In the case of MCT12 this substrate is creatine (13), a spatial and temporal energy buffer usually found in tissues with high energy demands such as skeletal and cardiac muscle, brain and retina (27). Suggested roles of creatine in the lens may involve an energy pathway alternative to oxidative phosphorylation by rapidly providing and storing excess energy as well as antioxidant activity through its capability to scavenge free radicals (28) and protection against UV radiation, a risk factor for cataract (29). Consequently, mutations in MCT12 that interfere with chaperone CD147 interaction or creatine docking and release could lead to cataract formation. Alternatively, pathomechanisms involving aggregation of misfolded proteins as well as altered response to cellular stress, as has been shown for a premature stop codon mutation in MCT12 (17), are possibilities. To understand the complexity of MCT12 (CRT2) function, we screened DNA from patients with ARC and identified and investigated sequence variants in MCT12 to shed light on its pathomechanism with emphasis on creatine uptake and potential rescue via its chaperone CD147.

Results

Mutation screening in the protein-coding region of SLC16A12

We screened 877 patients who were diagnosed with age-related cataract (ARC) (Table 1) for sequence variants in the coding region and canonical splice sites of exons 3 to 8 of *SLC16A12* and identified 13 different heterozygous sequence variants in 15 patients (Table 2), yielding approximately a 1: 60 frequency of affected patients. Only one variant mapped to the canonical splice site c.200 + 3 A > G (IVS3) (patient ID #1), while the others localized to the coding region. No clustering of variants to a particular region of the gene was found (Table 2). Five variants were novel [c.178 A > G: p.Ile60Val (patient ID #3), c.200 + 3 A > G (patient ID #1), c.228 C > G: p.Phe76Leu (patient ID #4), c.1184 C > A: p.Pro395Gln (patient ID #12), and c.1359 T > G: p.Ser453Arg (Patient ID #15)]. The other eight were very rare in the European (<0.002) and Asian (<0.0009) Exome Aggregation Consortium (ExAC) data base (Table 3). Four variants did not cause a change in amino acid [p.Ala53Ala (patient ID #2), p.Thr87Thr (patient ID #5), p.Ile178Ile (patient ID #10), and p.Ala410Ala (patient ID# 14)], while for eight variants a non-synonymous amino acid change was the consequence of the nucleotide substitution [p.Ile60Val (patient ID #3), p.Phe76Leu (patient ID #4), p.Thr136Met (patient IDs #6, 7, 8), p.Ser158Pro (patient ID #9), p.Gly205Val (patient ID #11), p.Pro395Gln (patient ID #12), p.Ser406Cys (patient ID #13), and p.Ser453Arg (patient ID #15)]. We applied algorithms to assess potential effects on gene expression with primary focus on splicing for these variants (Supplementary Material, Table S1). For the c.200 + 3 A > G (IVS3) variant a splice donor site is likely affected and for the four synonymous amino acid changes altered exonic splicing enhancer (ESE) binding sites were predicted. Variants leading to non-synonymous amino acid changes were also predicted to have effects on gene expression, mostly affecting ESE binding sites and in one case a weakly activated cryptic donor site. Among the variants leading to an amino acid exchange, of particular interest is the novel variant p.Ser453Arg, for which a stronger splice acceptor site as well as a novel strong cryptic splice donor site were predicted (Supplementary Material, Fig. S1). Usage of the new donor site is predicted to lead to skipping of exon 7 and the first 70 nucleotides of exon 8, which would result in a premature termination after 8 amino acids.

Considering the evolutionary relations, all variants appeared highly conserved. Together with dramatic changes in amino acid characteristics (Table 3) the alterations are likely to pose a negative effect on protein function. Application of five algorithms (AlignGVGD, SIFT, MutationTaster2, PolyPhen2 and UMD) aiming to assess pathogenicity yielded varying predictions (Supplementary Material, Table S1); not a single variant was predicted to be disease causing by all five algorithms. All but one variant [rs190323395 (c.407 C > T; p.Thr136Met)], were found only once in the patient cohorts. This exception was detected in three patients, all from the Malayan Singapore cohort (patient IDs #6, 7, 8) (Table 2). The frequency of this variant in the Asian population is very low (<0.00001) and hence is not likely to represent a common risk factor for ARC in this ethnic group. An alternative explanation of genetic relatedness among the three patients is not necessarily given as the genomic DNA of one of the three patients carries a distinct SNP rs3740030 allele. Four of the five prediction algorithms suggested a pathogenic consequence for this variant (Supplementary Material, Table S1).

Table 1. Description of study. Listed are the origin, source and number of patients

Origin of sample	Clinic, cohort/referring clinician	No. patients
Canada	Hospital for Sick Children/E. Heon	24
Switzerland	Hopital ophtalmique Jules-Gonin Sion/F. Munier	340
Singapore	Singapore Malay Eye Study (SiMES)	192
Singapore	Singapore Indian Eye Study (SINDI)	192
Singapore	Singapore Chinese Eye Study (SCES)	129

Table 2. Rare *SLC16A12* sequence variants identified in cataract patients. Patients' identifiers (ID) were assigned at random. The source and ethnicity of the cohorts were from Switzerland (CH), Canada and Singapore. The latter cohort could be specified to the following ethnicities: SINDI (Indian), SCES (Chinese) or SiMES (Malay). When ethnicity information was not available, it is marked as (na). Variant information included exon location, cDNA and amino acid (aa) substitution

patient ID	source/ethnicity	SLC16A12 exon	cDNA change	aa substitution
1	CH/na	3	c.200 + 3 A>G (IVS3)	none
2	Singapore SINDI (Indian)	3	c.159T>C	p.Ala53Ala
3	CH/na	3	c.178A>G	p.Ile60Val
4	Singapore SCES (Chinese)	4	c.228C>G	p.Phe76Leu
5	Singapore SCES (Chinese)	4	c.261G>A	p.Thr87Thr
6	Singapore SiMES (Malay)	5	c.407C>T	p.Thr136Met
7	Singapore SiMES (Malay)	5	c.407C>T	p.Thr136Met
8	Singapore SiMES (Malay)	5	c.407C>T	p.Thr136Met
9	CH/na	6	c.472T>C	p.Ser158Pro
10	CH/na	6	c.534C>T	p.Ile178Ile
11	Singapore SINDI (Indian)	6	c.614G>T	p.Gly205Val
12	Singapore SiMES (Malay)	7	c.1184C>A	p.Pro395Gln
13	Canada/na	7	c.1217C>G	p.Ser406Cys
14	Singapore SiMES (Malay)	7	c.1230G>A	p.Ala410Ala
15	CH/na	8	c.1359T>G	p.Ser453Arg

Table 3. Frequency of rare variants in population and their effect on MCT12. Change in cDNA and amino acid is related to effects on MCT12 as change in amino acid characteristics and the closest conserved species. SNP nomenclature is given where applicable; novel variants are indicated by minus (–). Frequencies in European and Asian population are taken from exome aggregation consortium (ExAc) database

			ExAC Frequency			effect on MCT12 and conservation	
Change in cDNA	Change in amino acid	dbSNP	European	South Asian	East Asian	change in amino acid characteristics	closest conserved species
c.200 + 3 A>G (IVS3)	none	–	–	–	–	none	
c.159T>C	p.Ala53Ala	rs577369974	0.00000	0.00091	0.00000	none	
c.178A>G	p.Ile60Val	–	–	–	–	nonpolar to nonpolar	Chicken
c.228C>G	p.Phe76Leu	–	–	–	–	nonpolar to nonpolar	Tetraodon
c.261G>A	p.Thr87Thr	rs761769735	0.00000	0.00000	0.00093	none	
c.407C>T	p.Thr136Met	rs190323395	0.00015	0.00000	0.00000	hydroxyl to nonpolar	Baker's yeast
c.472T>C	p.Ser158Pro	rs150800688	0.00197	0.00000	0.00000	hydroxyl to nonpolar	Frog
c.534C>T	p.Ile178Ile	rs192441993	0.00000	0.00000	0.00081	none	
c.614G>T	p.Gly205Val	rs778507843	0.00000	0.00006	0.00000	nonpolar to nonpolar	Fruitfly
c.1184C>A	p.Pro395Gln	–	–	–	–	nonpolar to amide	Fruitfly
c.1217C>G	p.Ser406Cys	rs145362501	0.00000	0.00018	0.00000	hydroxyl to sulfhydryl	Chicken
c.1230G>A	p.Ala410Ala	rs748432746	0.00000	0.00006	0.00000	none	
c.1359T>G	p.Ser453Arg	–	–	–	–	hydroxyl to basic	Tetraodon

Table 4. Risk factor analysis of SNP rs374003o. Patients (cases) and ethnically matching controls for the three tested ethnicities are listed. Major (T) and minor (G) allele frequency is given including the percent (%) of the minor allele as well as minor allele frequency (MAF). P value was derived from calculations for odds ratio. Significance level is 0.05

Patients and controls	T	G	total	%G	MAF	p
SiMES (Malay) cases	286	86	372	23.12	0.2312	0.5967
SiMES (Malay) controls	1721	555	2276	24.40	0.2440	
SINDI (Indian) cases	378	6	384	1.56	0.0156	0.3222
SINDI (Indian) controls	1759	43	1802	2.39	0.0239	
SCES (Chinese) cases	199	55	254	21.65	0.2165	0.5657
SCES (Chinese) controls	1410	355	1765	20.11	0.2011	

In addition to the very rare variants described above, SNP rs3740030 occurs at higher frequency in the general population (European including Finnish: 0.1139; South Asian: 0.0238; East Asian: 0.2235). In a previous study, we reported evidence that the minor allele of rs3740030 is a risk factor for ARC, using our Swiss control population (14). Analysis of these SNP alleles in the ARC patient samples from Singapore revealed a dramatic difference in frequency within the three ethnic groups but based on the frequencies within their respective ethnical population the existence of a risk or protective factor was not supported ($P = 0.6467$ for the Malays; $P = 0.4237$ for the Indian and $P = 0.6242$ for the Chinese) (Table 4).

Functional characterization of amino acid substitutions in MCT12

The function of the variants with non-synonymous amino acid changes was assessed by measuring creatine uptake in the heterologous expression system of *Xenopus laevis* oocytes, where the identification of creatine as a substrate for MCT12 had been performed and uptake conditions had been established. Variants p.Ser158Pro, p.Gly205Val, p.Pro395Gln, p.Ser406Cys, and p.Ser453Arg showed statistically significantly reduced creatine uptake compared to reference MCT12 (Fig. 1A, Supplementary Material, Table S2). Experimental conditions for substrate uptake into frog oocytes require a temperature of 24° C. To address a potential temperature sensitive effect, those variants with a creatine uptake reduction of 50% or more (p.Ser158Pro, p.Gly205Val, p.Pro395Gln, and p.Ser453Arg) were tested at 37° C in human HEK293T cells, a temperature more physiologically relevant to humans. A highly comparable uptake profile was observed with around 50% reduction for variant p.Ser158Pro, 85% for p.Pro395Gln and up to 97% reduction for p.Gly205Val and p.Ser453Arg (Fig. 1B). Creatine uptake in the latter two variants was statistically indistinguishable from the non-injected oocytes ($P = 0.0801$ and $P = 0.1407$, respectively) and non-transfected HEK293T cell controls ($P = 0.2435$ and $P = 0.1757$, respectively). In HEK293T cells, interference from the natively expressed sodium dependent creatine transporter 1 (CRT1, *SLC6A8*) has been ruled out by the use of a sodium free uptake buffer.

To gain better understanding of the underlying reason for the reduced uptake, we analyzed membrane localization of the MCT12 mutants after injection into frog oocytes or transfection of HEK293T cells and compared it to the reference. An antibody against the C-terminal amino acids (499: 516) of MCT12 was generated and tested for specificity. Western blots from injected frog oocyte lysates showed a single strong band of approximately 37 kD in size, that is not seen in non-injected controls (Supplementary Material, Fig. S2). The difference to the expected size of MCT12 (53.4kD) might be due to detergent effects, a phenomenon not uncommonly observed for membrane proteins (30). Alternatively, or in addition, protein modifications may also play a role here, as was described for alpha crystallins (31) or S-nitrosation of MCT1 (32). This verified anti-MCT12 antibody was used to investigate MCT12 membrane localization by immunofluoresence. Oocytes injected with reference or mutant MCT12 displayed an MCT12 specific signal at the cell membrane for all variants except for p.Gly205Val and p.Ser453Arg with severe reduction in creatine uptake. The mutation p.Pro395Gln, which also leads to a strong reduction in creatine uptake, did localize to oocyte membranes (Fig. 2). As expected, no signal was detected in non-injected (NI) oocytes. Immunocytochemistry of transfected HEK293T cells revealed the presence of MCT12 for all constructs, although no strict membrane localization was observed (Fig. 2).

Possible functional rescue through exogenous supplementation of CD147

To assess interactions between MCT12 mutations and the molecular chaperone we investigated the effect of exogenous human CD147 on creatine uptake by reference MCT12 and the respective mutations in frog oocytes and HEK293T cells. It was shown previously that endogenous *X. laevis* CD147 is sufficient to localize MCT12 to the oocyte membrane and facilitate creatine transport (13,33). However, this might not be the case for the mutations p.Gly205Val and p.Ser453Arg as human and frog CD147 only share 45% homology. In the frog oocyte system the addition of human CD147 does not seem to have a statistically significant effect on either creatine uptake (Supplementary Material, Fig. S3) or membrane localization (Supplementary Material, Fig. S4). In the human cell culture system three different creatine uptake time points, 1, 5 and 10 min, in absence and presence of exogenous CD147 were tested. As expected, for cells transfected with reference MCT12 without additional CD147 the intracellular creatine concentration is rising with increasing incubation time for creatine uptake (Fig. 3A). The addition of exogenous CD147 to MCT12 led to statistically significantly reduced creatine uptake at 5 and 10 min of uptake time ($P = 0.0018$ and $P = 0.0151$ respectively) (Fig. 3A, Supplementary Material, Table S3). In contrast, overexpression of the molecular chaperone CD147 significantly improves the uptake of creatine by the variants p.Ser158Pro, p.Gly205Val and p.Pro395Gln at all tested uptake time points (Fig. 3B–D, Supplementary Material, Table S3). Measured values for creatine uptake of variant p.Ser453Arg in absence or presence of exogenous CD147 were below the limit of detection (data not shown in graph Fig. 3, but in

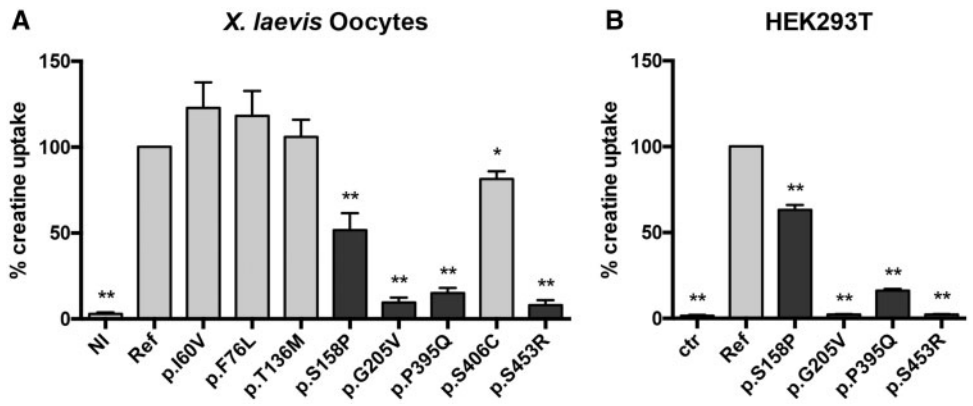

Figure 1. Functional analysis of sequence variants in MCT12. Creatine uptake was measured in (**A**) *Xenopus laevis* frog oocytes at 24 °C and in (**B**) HEK293T cells at 37 °C after incubation with creatine for 10 min. Uptake is expressed in percent relative to the reference sequence (Ref). Non-injected oocytes (NI) and non-transfected (ctr) HEK293T cells show endogenous background. In oocytes, the eight identified non-synonymous cataract associated variants were tested. Statistical significance was determined using unpaired, two-tailed *t*-tests with Welch's correction in comparison to the reference (Ref) values (*$P \leq 0.05$, **$P \leq 0.01$). Error bars reflect standard error of the mean (SEM). Mean values contain 5 to 16 different oocytes from at least 3 different uptake experiments with oocytes from different frogs. HEK293T cell uptake assays were performed with quadruple repeats and each condition was tested three times. In the frog oocytes sequence variants with dark bars indicate a reduction of 50% or more creatine uptake relative to Ref. These mutations were tested in HEK293T cells.

Supplementary Material, Table S3). While creatine uptake was generally increased in the presence of additional CD147, the difference between absence and presence of CD147 at each time point was not constant. This difference was visualized in the line graph (Fig. 3E), The most positive changes upon CD147 addition could be seen for variant p.Gly205Val (Fig. 3E, Supplementary Material, Table S3). This rescue effect becomes statistically significantly greater with increasing creatine uptake time (for all comparisons $P < 1.0E\text{-}9$). A very similar profile can be seen for variant p.Pro395Gln, although the total increase of creatine uptake is not as strong (for all comparisons $P < 1.0E\text{-}8$). Variant p.Ser158Pro did not show strong sensitivity to uptake time as can be seen in the almost linear slope of the line graph, and in the fact that only the difference between 1 and 5 min is statistically significant ($P = 0.0036$) (Fig. 3E, Supplementary Material, Table S3).

The effects of human CD147 overexpression on the localization pattern of MCT12 within HEK293T cells was examined through double staining with anti-CD147 and anti-MCT12 antibody (Fig. 4, Supplementary Material, Fig. S5). Supplementation of CD147 seems to improve membrane localization in cells transfected with reference or mutant constructs. As expected, some endogenous CD147 expression was detected by the staining, but no endogenous MCT12 expression is visible.

Discussion

The collection of very rare variants reported here did not contain deletions, insertions or frameshift effects. Little less than half of them (40%) had not been reported previously in sequence variant databases. All but one of the variants maps to the coding region, suggesting that functional alteration of the protein with possible consequences in localization, protein-protein interactions or substrate transport are impacted and may ultimately lead to the disease. Certainly, screening the coding regions presents a bias towards these kinds of variants. In addition to causing potential disruption of transporter function, some of the coding region mutations may also lead to exonic splicing enhancer (ESE) sequence alterations, and are thereby predicted to affect gene expression (34). An estimation of the extent of ESE effect has been reported previously (35) where a combined approach of bioinformatics and experimental evidence showed that about 25% of coding region mutations that cause human disease are likely due to exon skipping involving both, exonic splicing enhancers (ESE) and silencers (ESI). In our collection, three of the four synonymous coding region variants are predicted to alter splice sites with pathogenic consequences. Among the non-synonymous alterations that we found, all are predicted to alter splice sites but their validity needs to be tested. A highly probable case may present the mutation c.1359 T > G, p.Ser453Arg, where a predicted frame shift with premature termination may have important consequences on function within the human lens. For the three non-synonymous mutations that did not display deficiencies in creatine uptake in the *Xenopus laevis* oocyte system predicted splice defects could be the mechanism of pathogenicity. Similarly, mutation c.1217 C > G showed statistically significant reduction of creatine uptake in the oocyte system, but not below the 50% level, the predicted gain of an ESE site may contribute to pathogenicity.

The impact of sequence variants on protein function was estimated with the help of five prediction algorithms (AlignGVGD, SIFT, PolyPhen2, MutationTaster2 and UMD), all based on various features of the protein, like the degree of sequence homology, 3 D-folding, evolutionary conservation, and functional homologies. The validity of such predictions will come from functional assays. In our cases, half of the non-synonymous amino acid variants resulted in more than 50% reduction of creatine uptake. A most striking contrast was noticed for p.Ser453Arg, which is evolutionary highly conserved, and although only two of the five algorithms predicted pathogenicity, function is completely abolished in both model systems. A combination of the potential splice defect discussed above with the observed defect in substrate uptake at the protein level and lack of membrane localization seems a likely cause for the pathogenicity. Not surprisingly, addition of CD147 did not rescue this defect. Unfortunately, patient's material was not available for further testing.

Given that for the here reported mutations the changes in biochemical properties of the substituted amino acid are strong and the affected amino acids display evolutionary conservation, it is surprising that not a single mutation was predicted

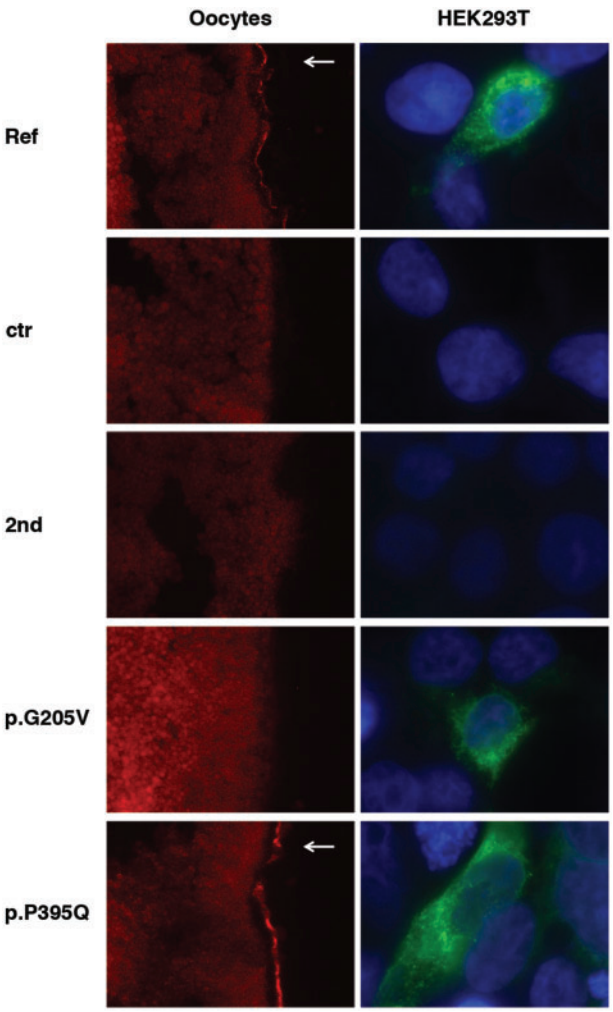

Figure 2. Localization of MCT12 and variants. Immunofluorescence of injected *X. laevis* oocytes (left) or transfected HEK293T cells (right) with antibody against the C-ter of MCT12 (red in oocytes, green in HEK293T) and DAPI (blue, only in HEK293T). Reference sequence and representative variants p.G205V and p.P395Q are shown. As controls non-injected oocytes and non-transfected cells are shown as well as a secondary antibody control of the reference sequence. Arrows point to membrane staining.

pathogenic by all programs. Such contrasting results of prediction and experimental evidence have been previously reported and need consideration in diagnostics from NGS data (36,37).

p.Gly205Val is another variant that did not localize to the oocyte membrane. The substitution of glycine with valine could alter the structure of the respective resident transmembrane domains, either directly or indirectly by possibly preventing required or enabling novel molecular interactions, for example with the chaperone CD147. When glycine, which has rich conformational flexibility, is substituted by the larger amino acid valine, disruption of the secondary structure of the protein is likely. Alternatively, a process known as unfolded protein response (UPR) could be initiated by the mutation as has been shown for another mutation in *SLC16A12* (17) and also for mutations in collagen IVa, leading to cataract (38). p.Ser158Pro, p.Pro395Gln and p.Ser406Cys are mutations in which creatine uptake was reduced, but the protein MCT12 can be found at the oocyte membrane. A partial translocation defect cannot be excluded though, as our membrane localization assay was not quantitative. Substitution of the serine, and thereby loss of a potential phosphorylation site, may contribute to the defective uptake, as was shown for the glutamine transporter SN1 (*SLC38A3*), where phosphorylation of an N-terminal serine by protein kinases α and γ is essential for membrane trafficking (39). Alternatively, the serine to proline or cysteine substitution could affect creatine binding, rendering transport less efficient. Proline residues generally tend to be non-reactive but allow conformational changes that show flexible behavior in different physiological states (40). Substitution with the polar glutamine in p.Pro395Gln, which tends to interact with other polar amino acids of adjacent proteins, may lead to novel protein-protein interactions. Such novel interactions have been described between the intracellular protein carbonic anhydrase II and MCT1 or MCT4 monocarboxylate transporters, leading in those examples to increased function (41).

In our initial choice of experimental model, the heterologous *Xenopus laevis* oocyte system, temperature sensitive effects leading to misprocessing have been reported for mutations in the membrane protein HERC channel (42) and the most frequently occurring mutation (ΔF508) in the cystic fibrosis gene *CFTR*, which functions better at lower temperatures (43). To assess whether such temperature sensitive responses also account for the MCT12 mutations analyzed here, all constructs were also tested in human cells. As the uptake results were comparable in both systems, temperature sensitive effects on the variants seemed unlikely. In contrast, for the interaction between MCT12 and the chaperone CD147 a species-specific effect becomes apparent, as the addition of CD147 only yielded rescued uptake in human cells and not in frog oocytes. A similar situation has been reported in the case of chaperone Hsp70 and the ΔF508 mutation in CFTR (44), and effects such as these could be, but are not necessarily, related to temperature. Interestingly, sensitivity to the time of uptake in dependence of chaperone CD147 supply became quite apparent; while the reference construct displayed reduced uptake over time from 1 to 10 min, the mutants conversely improve substrate uptake. A possible explanation might involve the bidirectional nature of creatine transport by MCT12 (13). Further, correct stabilization of MCT12, facilitated by CD147, could be a requirement for creatine transport. This stabilization may have a mutant-specific effect. Overexpression of CD147 may also explain these observations. Using cells where the endogenous CD147 is silenced may shed light on this possibility. Furthermore, we cannot exclude whether additional chaperone molecules other than CD147 might be necessary to support correct function of MCT12. Embigin, a close homolog of CD147, is one possible candidate as it is the chaperone for MCT2 (19). In support MCT1, whose general chaperone is CD147, was found to also interact with embigin in rat erythrocytes (45). It should be noted that although we were able to test function via substrate uptake, we cannot exclude effects on substrate efflux or other, possibly more subtle physiological conditions. The variants for which no uptake deficiency was found (p.Ile60Val, p.Phe76Leu and p.Thr136Met) could belong into that group due to inertia of the specific amino acid exchange or the location of the affected amino acid within the transporter that is unrelated to substrate uptake. We cannot completely rule out that these variants may be unrelated to ARC as their low frequency does not allow for genetic association tests in populations.

One of our aims was to assess how frequent sequence variants in *SCL16A12* can be found in patients with ARC. With an approximately 1 in 60 frequency, *SLC16A12* is next to *EPHA2* (10) among the most frequently affected genes. Combination of this

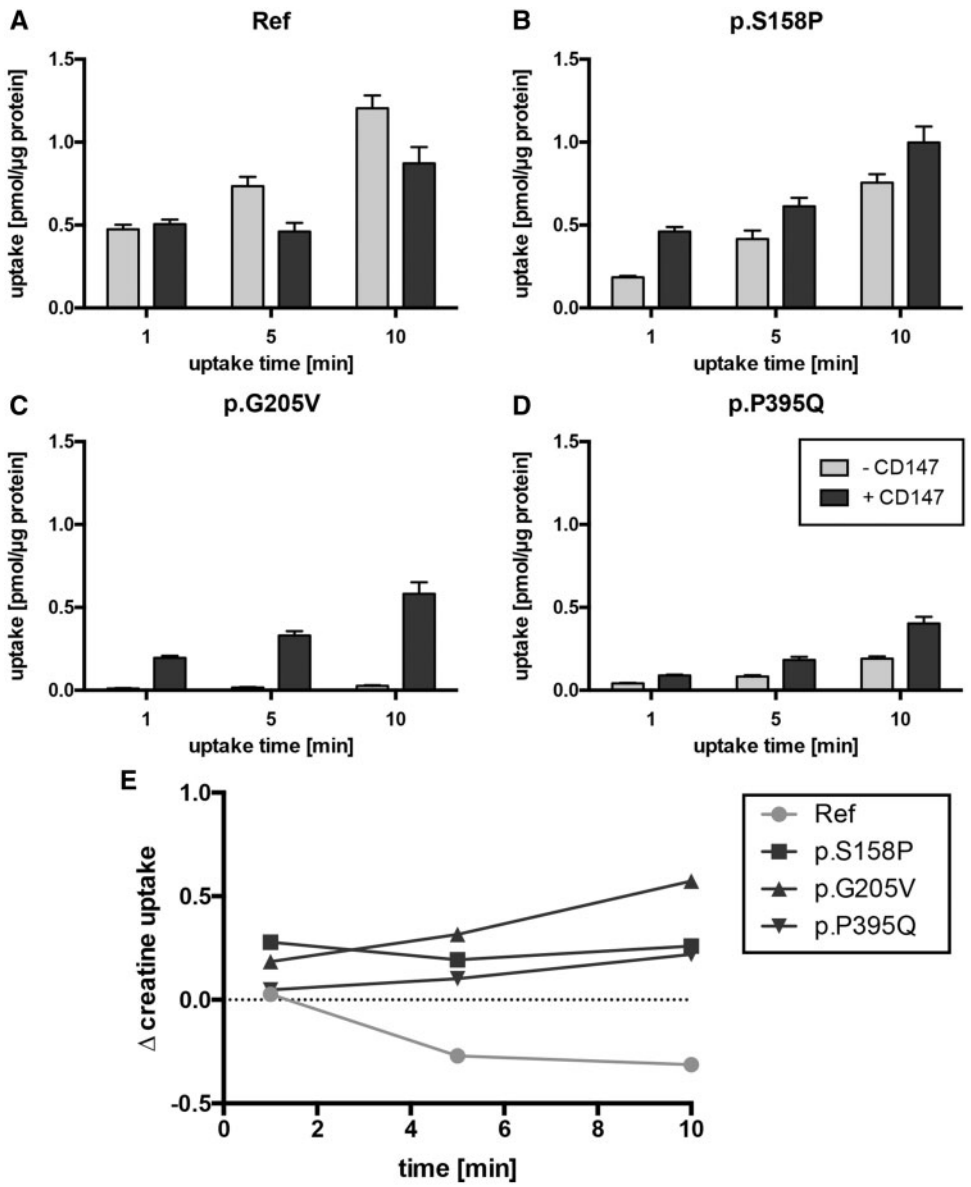

Figure 3. Influence of CD147 on creatine uptake in HEK293T cells. Uptake of creatine in pmol/µg protein is shown in bar graphs for the reference sequence (Ref) (**A**) and variants p.S158P (**B**), p.G205V (**C**) as well as p.P395Q (**D**) in the absence (light bar) and presence (dark bar) of exogenous CD147 during 1, 5 or 10 min of uptake. Unpaired, two-tailed t-test with Welch's correction was applied. CD147 overexpression leads to a statistically significant increase in creatine uptake for all three shown mutants at all three time points and a statistically significant decrease for the reference at 5 and 10 min. The difference between without and with CD147 is displayed in the line graph (**E**). Error bars indicate standard error of the mean. Numerical data are given in Supplementary Material, Table S4. Same experiments were performed for variant p.S453R but as all data points were below the limit of quantification (Supplementary Material, Table S4), no bar or line graph display is given.

frequency with the presence of MCT12 transporter and its chaperone CD147 in human ocular lens (Supplementary Material, Fig. S6) may justify searches for non-invasive treatment methods, alternatively to the commonly performed surgery. One approach could employ supplements of creatine, an approach that was successful in mice with X-linked *SLC6A8* (CRT1) mutations (46). As creatine supplements in humans have been approved by the Food and Drug Administration (FDA) in the USA, a first hurdle has been taken for investigations in humans. Another approach addresses the effects of molecular chaperones. Here, we could demonstrate a positive response to cataract-associated mutation-induced creatine uptake deficiencies by supplying exogenous CD147 in mammalian cell culture. The mechanism of the partial rescue of mutations p.Ser158Pro, p.Gly205Val, and p.Pro395Gln is not yet understood. It is interesting that both, mutations leading to membrane localization or not, can be rescued. Likely, the mutations map to sites within MCT12 that are important for interaction with CD147 causing sub-optimal conditions for proper trafficking. Over-abundance of CD147 appears to overcome this problem. The here reported partial rescue gives encouraging signals for further studies of optimization. In previous studies, effects of chaperone treatments on different diseases provided promising results. It was shown that overexpression of chaperone Hsp70 led to improved interaction with the ΔF508 mutant in the cystic fibrosis gene *CFTR* (44). In another example, application of small corrector molecules (VX-809) could rescue processing mutants in the Stargardt eye disease ABCA4 protein (47). A note of caution

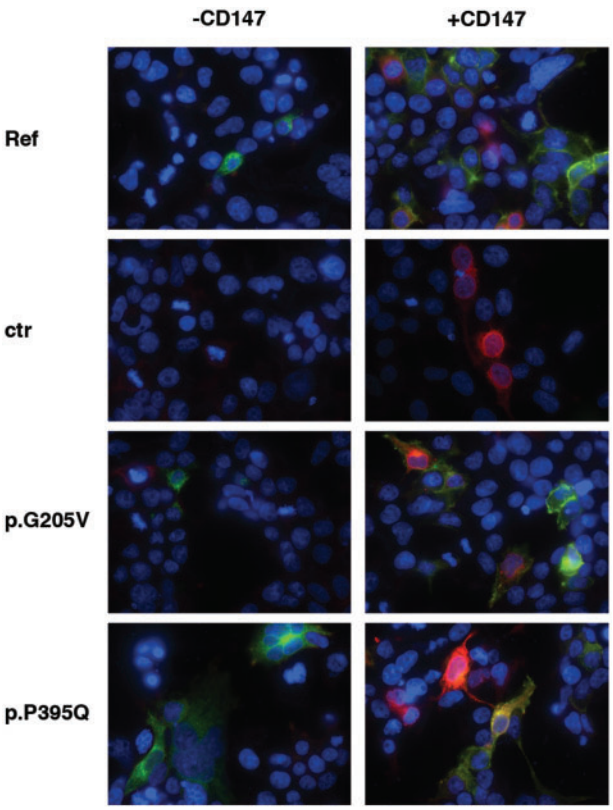

Figure 4. Localization of MCT12 and variants with and without exogenous CD147. Immunofluoresence of transfected HEK293T cells with antibody against MCT12 (green), CD147 (red) and DAPI (blue). Shown are cells transfected with reference sequence as well as variants p.G205V and p.P395Q without (left) and with (right) addition of exogenous CD147. Non-transfected cells were used as control.

is based on the fact that chaperones usually play several important roles in cellular processes and hence alteration of its concentration may lead to unwanted responses.

Taken together, our screen for pathogenic variants in *SLC16A12* yielded a collection of sequence variants of which about half displayed functional deficiency with respect to substrate uptake. This was observed in two evolutionary and experimentally rather distant models: frog oocytes and human cells. The functional deficiency could be partially rescued in the human model by addition of chaperone CD147. Further investigations in potential non-invasive treatments are encouraged.

Materials and Methods

Patients with cataracts

Patients diagnosed with age-related cataract were (i) from Switzerland (340 patients diagnosed by Dr. F. Munier), (ii) from Canada (24 patients diagnosed by Dr. E. Heon) and (iii) from Singapore (513 subjects with age-related cataracts from three different ethnic backgrounds; 192 Singaporean Malays (48–50), 192 Singaporean Indian (51,52) and 129 Singaporean Chinese (52) from the Singapore Epidemiology of Eye Diseases Study (53) (Table 1). All patients from Singapore had mostly severe nuclear age-related cataract with a small subset (approximately 20%) that had additional cortical and/or additional subcapsular cataract. Participation at the different sites was approved by the respective ethics regulatory bodies and all patients gave written informed consent. Experiments respected the principles expressed in the Declaration of Helsinki.

SLC16A12 DNA sequence analysis

Genomic DNA from venous blood was amplified using primers for coding exons 3 to 8 of *SLC16A12* gene (Supplementary Material, Table S4) (Entrez ID 387700, NM_213606.3). PCR amplification and Sanger sequencing were performed as described (14,16). Initially, 50 ng genomic DNA was amplified in a 25 μl reaction volume. Tests with 1-5 ng genomic DNA in 10 μl reaction volume yielded equivalent results and hence, the latter conditions were chosen for most of the PCR reactions. Electropherograms were evaluated using SeqScape (ABI) software. DNA samples showing variants were subjected to a second PCR and sequencing reaction. Variants were annotated using Alamut-Visual (Interactive Biosoftware). For missense mutations, five common algorithms (SIFT (54), MutationTaster2 (55), Align GVGD (56,57) PolyPhen2 (58) and UMD (59)) were applied to predict pathogenicity. Genotype data for SNP rs3740030 from the control groups from Singapore were provided by the Singapore Eye Research Institute.

Cloning and *in vitro* transcription

SLC16A12 reference (ENST00000341233; protein Q6ZSM3; 486 amino acids) cDNA clone in vector KSM for *Xenopus laevis* oocyte injections has been described (13). This clone was used for site directed mutagenesis (60) to generate constructs with the cataract associated sequence variants (Supplementary Material, Table S4). To eliminate the template DNA, amplification products were digested with methylation sensitive restriction enzyme *Dpn*I (Fermentas). Clones were verified by Sanger DNA sequencing. DNA of confirmed plasmids were linearized using *Not*I, *Bst*XI or *Sac*II, followed by *in vitro* transcription of 1 μg linearized DNA using the MEGAscript T3 High Yield Transcription kit (AMbion), including G(5')ppp(5')G RNA Cap structure analog (New England Biolabs) in a volume ration of 1: 3 with GTP. Quality and quantity of RNA were determined using the Agilent RNA 6000 Nano kit (Agilent). All nucleotide primers were synthesized at Microsynth, Balgach, Switzerland.

For transfection of HEK293T (GE healthcare Bio-Sciences AB) cells, the *SLC16A12* reference and sequence variants in the BlueScript derived vector KSM (see above) were cloned into the bicistronic vector pIRES2-EGFP (Adgene). Both plasmids were linearized using restriction enzyme *Eco*RI and *Xho*I (ThermoScientific) and resulting fragments were gel extracted with the NucleoSpin® Gel and PCR Clean Up kit (Macherey-Nagel). The pIRES-EGFP backbone and cDNA insert were ligated with T4 DNA ligase (Promega). Plasmid identity was confirmed by Sanger Sequencing. Clones containing cRNA of *BSG* (CD147; ENST00000333511; protein P35613; 385 amino acids) for *Xenopus laevis* oocyte injections as well as cDNA of *BSG* in the pIRES-EGFP vector for transfection of HEK293T cell culture were prepared as described above for *SLC16A12*.

Creatine uptake assay

Xenopus laevis oocytes, Injection procedure and uptake assays were performed as previously reported (13). For each MCT12 construct at least 10 oocytes from a given frog were injected with 25 ng/50 nl of *SLC16A12* RNA. Experiments were repeated 3 to 5 times with eggs from different frogs. For the constructs that

showed reduced uptakes a new *in vitro* transcription reaction was performed for another set of uptake experiments. Creatine uptake was calculated relative to uptake in oocytes injected with reference MCT12.

HEK cell culture, HEK293T cells were cultured in DMEM (Gibco by Sigma Life Science) [supplied with 10% FCS (Eurobio) and 1% pen/strep (Corning)] according to standard protocols. Uptake assays were carried out in 12-well plates. Cells were transfected using 1.2 μg of DNA and 3.6 μg PEI (polyethylenimine, Sigma) transfection agent. 48 h after transfection cells were washed in sodium free wash buffer (150 mM Cholin-Cloride, 10 mM HEPES pH7.4, 1 mM $CaCl_2$ $2H_2O$, 5 mM KCl, 1 mM $MgCl_2$ $6H_2O$, 10 mM Glucose, pH7.4) and kept for 5 min at 37 °C in the second wash. Per well 300 μl uptake solution (sodium free wash buffer supplied with 50 μM creatine hydrate and 0.1 μCi/ml ^{14}C-creatine (Hartmann Analytics, Braunschweig, Germany) was added and uptake was allowed for 1, 5 or 10 min at 37 °C. Cells were washed three times with ice cold wash buffer and lysed in 1% Triton X-100 (Roth) for 30 min. Background measurements were taken from the third wash. Radioactivity was measured using Emulsifier-Safe™ scintillation cocktail (PerkinElmer) and a Packard Tri-Carb liquid scintillation analyzer. Protein concentration of lysed cells was determined using the Pierce BCA Protein Assay (Thermo Fisher Scientific). From the obtained CPM (counts per minute) measurements uptake values were calculated in pmol creatine per μg of total protein. All uptakes were performed thrice and each uptake was carried out in quadruplicate repeats for every tested construct. Tests in HEK293T cells were performed in the absence and presence of exogenous CD147. The ratio of CD147 and MCT12 cDNA constructs for transfection was 1: 4. Statistical analysis through unpaired t-test with Welch's correction ($\alpha = 0.05$) and graphical displays were done in Prism 6 (Graphpad).

Immunofluorescence

Xenopus laevis oocytes, Five to ten oocytes per condition were prepared for cryosectioning as described (13) and sectioned at 10 μm using a cryomicrotome (Leica). Between steps sections were washed three times in PBS for 5 min. Sections were blocked for 1 h at room temperature in PBS containing 0.05% Triton-X 100 (PBST) and 2% BSA (Sigma). A primary polyclonal, affinity-purified, antibody against the C-terminal region (499: 516, nomenclature based on NP_998771.3 the long isoform of MCT12) of the human MCT12 was produced in rabbits (Thermo Fisher Scientific). Cryosections were incubated with primary anti-MCT12 antibodies diluted in PBST (1: 250) for 1 h at room temperature. Secondary goat anti-rabbit IgG Alexa Fluor© 488 or 568 antibody (Thermo Fisher Scientific) (1: 400 dilution in PBST) was applied for 1 h at room temperature. All slides were mounted using Fluoromount (Sigma) and kept at 4° C. Images were taken with the EVOS© FL microscope and processed with Photoshop CC (Adobe).

HEK cell culture, HEK293T cells were plated on Poly-L-Lysine (Sigma) treated 22 × 22 mm cover slips in 6-well plates. 48 h after transfection, cells were fixed in 4% PFA for 20 min, permeabilized with 0.2% Triton X-100 for 5 min and blocked in 5 mg/ml BSA in PBS for 30 min at room temperature. Between steps cells were washed three times in PBS. Primary antibodies against MCT12 (499: 516, Thermo Fisher Scientific) and CD147 (Ancell) were diluted to 1: 200 and 1: 400 respectively, in PBS with BSA. Cells were re-blocked for 30 min. Secondary Alexa Fluor© 488 goat anti-rabbit at 1: 400 and Alexa Fluor© 568 goat anti-mouse at 1: 800 dilutions (both Thermo Fisher Scientific) were applied for 45 min at 37° C. Cover slips were mounted using Fluoromount G® with DAPI (SouthernBiotech) and kept in the dark at 4 °C until microscopy with the EVOS FL Auto Cell Imaging System. Oocyte images were taken at 20x magnification; HEK293T cells at 60x magnification. Representative images were processed using Adobe Photoshop CC and may have been digitally magnified.

Human lens. A human lens from a cornea donor without obvious cataract provided by The University Hospital of Bern was frozen in liquid nitrogen and embedded in Tissue Tek (O.C.T. compound, Sakura Finetek, NL) medium without prior fixation on dry ice and sectioned at 8 μm using a cryomicrotome. The slides were stored at − 80° C. Cryosections were dried for 2 min at room temperature and fixed in 4% PFA for 10 min. Between steps, sections were washed three times in PBS for 5 min unless otherwise stated. The sections were blocked and treated with 2% BSA and 0.05% Triton-X in PBS. Primary antibody against MCT12 (1: 250, Thermo Fisher Scientific) and CD147 (1: 500, Sino Biological) were applied to sections for 1 h at room temperature. Cryosections were incubated with secondary antibody Alexa Fluor® 488 or 568 goat anti-rabbit at 1: 500 or 1: 400 dilution in blocking solution for 45 min in the dark. The slides were mounted using Fluoromount G® with DAPI and analysed with the EVOS FL Auto Cell Imaging System. Representative images were processed using Adobe Photoshop CC.

MCT12 antibodies and western blots

72 h post-injection cell extracts from 5 to 10 *Xenopus laevis* oocytes were prepared by the addition of 20 μl cold lysis solution (250 mM sucrose, 0.5 mM EDTA, 5 mM Tris base and freshly prepared protease inhibitors: PMSF (phenylmethylsulphonyl fluoride) 200 μg/ml and PIC (protease inhibitor cocktail) 1 mg/ml (all chemicals from Sigma-Aldrich)). The lysed oocytes were passed 10 times through a 25 G needle to homogenize the cells, followed by centrifugation at 100 g at 4 °C for 10 min. Protein concentration was determined using Pierce™ BCA protein assay kit (Thermo Fisher Scientific). Gel electrophoresis of 30 μg protein extract and molecular weight marker (Precision Plus Protein Dual Color Standards; BioRad) through 10% resolving acrylamide gel was performed followed by transfer to PVDF membrane using the Semi-Dry Transfer Cell (BioRad). Transfer efficiency was evaluated with Ponceau S (Sigma Aldrich). After blocking membrane overnight in 5% milk-TBST, hMCT12 primary antibody (1: 500 in blocking solution) was applied for 2 h at room temperature under constant rotation. Following washes, the secondary antibody (ECL™ anti-rabbit IgG HRP secondary antibody) (GE healthcare UK limited) was added in a 1: 10000 dilution. Membranes were developed using the Western Lightning Plus-ECL™ detection kit (PerkinElmer) according to manufacture's specifications and visualized with the Bio-Rad Imager (ChemiDoc XRS+ with Image Lab Software).

Web sites for sequence information and prediction programs

Alamut Visual vs2.7.2, a mutation analysis software (http://www.interactive-biosoftware.com/alamut-visual/). Within Alamut, programs to predict splice defects (Splice Site Finder-like, MaxEntScan, NNSPLICE, GeneSplicer, Human Splicing Finder as well as ESE Predictions with ESEfinder and RESCUE-ESE) have been used. Predictions for pathogenicity: Polyphen2 (http://genetics.

bwh.harvard.edu/pph2/), SIFT (http://sift.bii.a-star.edu.sg/), MutationTaster2 (http://www.mutationtaster.org/), Align GVGD (http://agvgd.hci.utah.edu/agvgd_input.php), umd-predictor http://umd-predictor.eu/ Collection of variants: http://exac.broadinstitute.org/, https://www.ncbi.nlm.nih.gov/snp/, http://cancer.sanger.ac.uk/cosmic DNA and protein sequence information: Genecards http://www.genecards.org/and NCBI http://www.ncbi.nlm.nih.gov/and UniProtKB http://www.uniprot.org/uniprot Statistics: http://vassarstats.net/tu.html for odds ratio calculations and GraphPad Prism 6 for uptake experiments. All web sites have been accessed last between February and June 2017.

Supplementary Material

Supplementary Material is available at *HMG* online.

Acknowledgements

We would like to thank Janitri Babu, Yachana Chakravarty, Ankita Choudhury, Pooja Gangras, Michel Bielecki and David Wenner (all from Institute of Medical Molecular Genetics, University Zurich, Switzerland) for help with DNA sequencing, cloning, creatine uptake and Western blots. Michele Visentin (Department of Clinical Pharmacology and Toxicology, University Zurich, Switzerland) for help with establishing creatine uptake assay in HEK293T cells.

Conflict of Interest statement. The authors declare no conflict of interest.

Funding

Swiss National Science Foundation Grant 320030_127558 (FLM, DFS), Hartmann Müller-Stiftung für Medizinische Forschung (BKG) and Novartis Stiftung für Medizinisch Biologische Forschung (BKG).

References

1. Shiels, A., Bennett, T.M. and Hejtmancik, J.F. (2010) Cat-Map: putting cataract on the map. *Mol. Vis.*, **16**, 2007–2015.
2. Shiels, A. and Hejtmancik, J. (2013) Genetics of human cataract. *Clin. Genet.*, **84**, 120–127.
3. Shiels, A. and Hejtmancik, J.F. (2015) Molecular genetics of cataract. *Prog. Mol. Biol. Transl. Sci.*, **134**, 203–218.
4. Ma, X., Jiao, X., Ma, Z. and Hejtmancik, J.F. (2016) Polymorphism rs7278468 is associated with Age-related cataract through decreasing transcriptional activity of the CRYAA promoter. *Sci. Rep.*, **6**, 23206.
5. Liao, R-f., Ye, M-J., Liu C-Y. and Ye, D-Q. (2015) An updated meta-analysis: risk conferred by glutathione S-transferases (GSTM1 and GSTT1) polymorphisms to age-related cataract. *J. Ophthalmol.*, 2015:**10**.
6. Sun, W., Su, L., Sheng, Y., Shen, Y. and Chen, G. (2015). Is there association between Glutathione S Transferases polymorphisms and cataract risk: a meta-analysis? *BMC Ophthalmol.*, **15,** 1–9.
7. Chi, X.X., Liu, Y.Y., Shi, S.N., Cong, Z., Liang, Y.Q. and Zhang, H.J. (2015) XRCC1 and XPD genetic polymorphisms and susceptibility to age-related cataract: a meta-analysis. *Mol. Vis.*, **21**, 335–346.
8. Liu, X.C., Liu, X.F., Hu, Z.D. and Li, Z.H. (2015) Polymorphisms of DNA repair genes XPD (Lys751Gln) and XRCC1 (Arg399Gln), and the risk of age-related cataract: a meta-analysis. *Curr. Eye Res.*, **40**, 676–682.
9. Wang, Y., Li, F., Zhang, G., Kang, L., Qin, B. and Guan, H. (2015) Altered DNA methylation and expression profiles of 8-Oxoguanine DNA glycosylase 1 in lens tissue from age-related cataract patients. *Curr. Eye Res.*, **40**, 815–821.
10. Jun, G., Guo, H., Klein, B.E., Klein, R., Wang, J.J., Mitchell, P., Miao, H., Lee K.E., Joshi, T., Buck, M. *et al.* (2009) EPHA2 is associated with age-related cortical cataract in mice and humans. *PLoS Genet.*, **5**, e1000584.
11. Shiels, A., Bennett, T.M., Knopf, H.L., Maraini, G., Li, A., Jiao, X. and Hejtmancik, J.F. (2008) The EPHA2 gene is associated with cataracts linked to chromosome 1p. *Mol. Vis.*, **14**, 2042–2055.
12. Yang, J., Luo, J., Zhou, P., Fan, Q., Luo, Y. and Lu, Y. (2013) Association of the ephreceptor tyrosinekinase-type A2 (EPHA2) gene polymorphism rs3754334 with age-related cataract risk: a meta-analysis. *PLoS One* **8**, e71003.
13. Abplanalp, J., Laczko, E., Philp, N.J., Neidhardt, J., Zuercher, J., Braun, P., Schorderet, D.F., Munier, F.L., Verrey, F., Berger, W. *et al.* (2013) The cataract and glucosuria associated monocarboxylate transporter MCT12 is a new creatine transporter. *Hum. Mol. Genet.*,
14. Zuercher, J., Neidhardt, J., Magyar, I., Labs, S., Moore, A.T., Tanner, F.C., Waseem, N., Schorderet, D.F., Munier, F.L. *et al.* (2010) Alterations of the 5'untranslated region of SLC16A12 lead to age-related cataract. *Invest. Ophthalmol. Vis. Sci.*, **51**, 3354–3361.
15. Halestrap, A.P. (2012) The monocarboxylate transporter family–Structure and functional characterization. *IUBMB Life*, **64**, 1–9.
16. Kloeckener-Gruissem, B., Vandekerckhove, K., Nürnberg, G., Neidhardt, J., Zeitz, C., Nürnberg, P., Schipper, I. and Berger, W. (2008) Mutation of solute carrier SLC16A12 associates with a syndrome combining juvenile cataract with microcornea and renal glucosuria. *Am. J. Hum. Genet.*, **82**, 772–779.
17. Castorino, J.J., Gallagher-Colombo, S.M., Levin, A.V., Fitzgerald, P.G., Polishook, J., Kloeckener-Gruissem, B., Ostertag, E. and Philp, N.J. (2011) Juvenile cataract-associated mutation of solute carrier SLC16A12 impairs trafficking of the protein to the plasma membrane. *Invest. Ophthalmol. Vis. Sci.*, **52**, 6774–6784.
18. Kirk, P., Wilson, M.C., Heddle, C., Brown, M.H., Barclay A.N. and Halestrap, A.P. (2000) CD147 is tightly associated with lactate transporters MCT1 and MCT4 and facilitates their cell surface expression. *EMBO J.*, **19**, 3896–3904.
19. Wilson, M.C., Meredith, D., Fox, J.E., Manoharan, C., Davies, A.J. and Halestrap, A.P. (2005) Basigin (CD147) is the target for organomercurial inhibition of monocarboxylate transporter isoforms 1 and 4: the ancillary protein for the insensitive MCT2 is EMBIGIN (gp70). *J. Biol. Chem.*, **280**, 27213–27221.
20. Wilson, M.C., Meredith, D. and Halestrap, A.P. (2002) Fluorescence resonance energy transfer studies on the interaction between the lactate transporter MCT1 and CD147 provide information on the topology and stoichiometry of the complex in situ. *J. Biol. Chem.* **277**, 3666–3672.
21. Grass, G.D. and Toole, B.P. (2015) How, with whom and when: an overview of CD147-mediated regulatory networks influencing matrix metalloproteinase activity. *Biosci. Rep.*, **36**, e00283.
22. Jiang, J.L. and Tang, J. (2007) CD147 and its interacting proteins in cellular functions. *Sheng Li Xue Bao*, **59**, 17–523.

23. Muramatsu, T. (2016) Basigin (CD147), a multifunctional transmembrane glycoprotein with various binding partners. *J. Biochem.*, **159**, 481–490.
24. Muramatsu, T. and Miyauchi, T. (2003) Basigin (CD147): a multifunctional transmembrane protein involved in reproduction, neural function, inflammation and tumor invasion. *Histol. Histopathol.*, **18**, 981–987.
25. Nahalkova, J. (2016) The protein-interaction network with functional roles in tumorigenesis, neurodegeneration, and aging. *Mol. Cell Biochem.*, **423**, 187–196.
26. Gallagher, S.M., Castorino, J.J., Wang, D. and Philp, N.J. (2007) Monocarboxylate transporter 4 regulates maturation and trafficking of CD147 to the plasma membrane in the metastatic breast cancer cell line MDA-MB-231. *Cancer Res.*, **67**, 4182–4189.
27. Wyss, M. and Kaddurah-Daouk, R. (2000) Creatine and creatinine metabolism. *Physiol. Rev.*, **80**, 1107–1213.
28. Sestili, P., Martinelli, C., Colombo, E., Barbieri, E., Potenza, L., Sartini, S. and Fimognari, C. (2011) Creatine as an antioxidant. *Amino Acids*, **40**, 1385–1396.
29. Löfgren S. (2017) Solar ultraviolet radiation cataract. *Exp. Eye Res.*, **156**, 112–116.
30. Rath, A., Glibowicka, M., Nadeau VG., Chen, G. and Deber, C.M. (2009) Detergent binding explains anomalous SDS-PAGE migration of membrane proteins. *Proc. Natl Acad. Sci. USA*, **106**, 1760–1765.
31. Yanshole, L.V., Cherepanov, I.V., Snytnikova, O.A., Yanshole, V.V., Sagdeev, R.Z. and Tsentalovich, Y.P. (2013) Cataract-specific posttranslational modifications and changes in the composition of urea-soluble protein fraction from the rat lens. *Mol. Vis.*, **19**, 2196–2208.
32. Diers, A.R., Broniowska, K.A., Chang, C.F., Hill, R.B. and Hogg, N. (2014) S-Nitrosation of monocarboxylate transporter 1: inhibition of pyruvate-fueled respiration and proliferation of breast cancer cells. *Free Radic. Biol. Med.*, **69**, 229–238.
33. Manoharan, C., Wilson, M.C., Sessions, R.B. and Halestrap, A.P. (2006) The role of charged residues in the transmembrane helices of monocarboxylate transporter 1 and its ancillary protein basigin in determining plasma membrane expression and catalytic activity. *Mol. Membr. Biol.*, **23**, 486–498.
34. Ward, A.J. and Cooper, T.A. (2010) The pathobiology of splicing. *J. Pathol.*, **220**, 152–163.
35. Sterne-Weiler, T., Howard, J., Mort, M., Cooper, D.N. and Sanford, J.R. (2011) Loss of exon identity is a common mechanism of human inherited disease. *Genome Res.*, **21**, 1563–1571.
36. Flanagan, S.E., Patch, A.M. and Ellard, S. (2010) Using SIFT and PolyPhen to predict loss-of-function and gain-of-function mutations. *Genet. Test Mol. Biomarkers*, **14**, 533–537.
37. Miosge, L.A., Field, M.A., Sontani, Y., Cho, V., Johnson, S., Palkova, A., Balakishnan, B., Liang, R., Zhang, Y., Lyon, S. *et al.* (2015) Comparison of predicted and actual consequences of missense mutations. *Proc. Natl Acad. Sci.*, **112**, E5189–E5198.
38. Firtina, Z., Danysh, B.P., Bai, X., Gould, D.B., Kobayashi, T. and Duncan, M.K. (2009) Abnormal expression of collagen IV in lens activates unfolded protein response resulting in cataract. *J. Biol. Chem.*, **284**, 35872–35884.
39. Nissen-Meyer, L.S., Popescu, M.C., Hamdani el, H. and Chaudhry, F.A. (2011) Protein kinase C-mediated phosphorylation of a single serine residue on the rat glial glutamine transporter SN1 governs its membrane trafficking. *J. Neurosci.*, **31**, 6565–6575.
40. Ri, Y., Ballesteros, J.A., Abrams, C.K., Oh, S., Verselis, V.K., Weinstein, H. and Bargiello, T.A. (1999) The role of a conserved proline residue in mediating conformational changes associated with voltage gating of Cx32 gap junctions. *Biophys. J.*, **76**, 2887–2898.
41. Klier, M., Andes, F.T., Deitmer, J.W. and Becker, H.M. (2014) Intracellular and extracellular carbonic anhydrases cooperate non-enzymatically to enhance activity of monocarboxylate transporters. *J. Biol. Chem.*, **289**, 2765–2775.
42. Ficker, E., Thomas, D., Viswanathan, P.C., Dennis, A.T., Priori, S.G., Napolitano, C., Memmi, M., Wible, B.A., Kaufman, E.S., Iyengar, S. *et al.* (2000) Novel characteristics of a misprocessed mutant HERG channel linked to hereditary long QT syndrome. *Am. J. Physiol. Heart Circ. Physiol.*, **279**, H1748–1756.
43. Denning, G.M., Anderson, M.P., Amara, J.F., Marshall, J., Smith, A.E. and Welsh, M.J. (1992) Processing of mutant cystic fibrosis transmembrane conductance regulator is temperature-sensitive. *Nature*, **358**, 761–764.
44. Chanoux, R.A. and Rubenstein, R.C. (2012) Molecular chaperones as targets to circumvent the CFTR defect in cystic fibrosis. *Front. Pharmacol.*, **3**, 137.
45. Poole, R.C. and Halestrap, A.P. (1997) Interaction of the erythrocyte lactate transporter (monocarboxylate transporter 1) with an integral 70-kDa membrane glycoprotein of the immunoglobulin superfamily. *J. Biol. Chem.*, **272**, 14624–14628.
46. Kurosawa, Y., Degrauw, T.J., Lindquist, D.M., Blanco, V.M., Pyne-Geithman, G.J., Daikoku, T., Chambers, J.B., Benoit, S.C. and Clark, J.F. (2012) Cyclocreatine treatment improves cognition in mice with creatine transporter deficiency. *J. Clin. Invest.*, **122**, 2837–2846.
47. Sabirzhanova, I., Lopes Pacheco, M., Rapino, D., Grover, R., Handa, J.T., Guggino, W.B. and Cebotaru, L. (2015) Rescuing trafficking mutants of the ATP-binding cassette protein, ABCA4 with small molecule correctors as a treatment for Stargardt eye disease. *J. Biol. Chem.*, **290**, 19743–19755.
48. Foong, A.W., Saw, S.M., Loo, J.L., Shen, S., Loon, S.C., Rosman, M., Aung, T., Tan, D.T., Tai, E.S. and Wong, T.Y. (2007) Rationale and methodology for a population-based study of eye diseases in Malay people: The Singapore Malay eye study (SiMES). *Ophthalmic. Epidemiol.*, **14**, 25–35.
49. Rosman, M., Zheng, Y., Lamoureux, E., Saw, S.M., Aung, T., Tay, W.T., Wang, J.J., Mitchell, P., Tai, E.S. and Wong, T.Y. (2012) Review of key findings from the Singapore Malay Eye Study (SiMES-1). *Singapore Med. J.*, **53**, 82–87.
50. Tan, A.G., Tay, W.T., Mitchell, P., Sandar, M., Aung, T., Saw, S.M., Wang, J.J. and Wong, T.Y. (2012) Prevalence of lens opacities in Asian Malays. *Ophthalmic. Epidemiol.*, **19**, 380–387.
51. Gupta, P., Zheng, Y., Ting, T.W., Lamoureux, E.L., Cheng, C.Y. and Wong, T.Y. (2013) Prevalence of cataract surgery and visual outcomes in Indian immigrants in Singapore: the Singapore Indian eye study. *PLoS ONE*, **8**, e75584.
52. Lavanya, R., Jeganathan, V.S., Zheng, Y., Raju, P., Cheung, N., Tai, E.S., Wang, J.J., Lamoureux, E., Mitchell, P., Young, T.L. *et al.* (2009) Methodology of the Singapore Indian Chinese Cohort (SICC) eye study: quantifying ethnic variations in the epidemiology of eye diseases in Asians. *Ophthalmic Epidemiol.*, **16**, 325–336.
53. Chua, J., Koh, J.Y., Tan, A.G., Zhao, W., Lamoureux, E., Mitchell, P., Wang, J.J., Wong, T.Y. and Cheng, C.Y. (2015) Ancestry, socioeconomic status, and age-related cataract in Asians: The Singapore Epidemiology of Eye Diseases Study. *Ophthalmology*, **122**, 2169–2178.

54. Kumar, P., Henikoff, S. and Ng, P.C. (2009) Predicting the effects of coding non-synonymous variants on protein function using the SIFT algorithm. *Nat. Protoc.*, **4**, 1073–1081.
55. Schwarz, J.M., Cooper, D.N., Schuelke, M. and Seelow D. (2014) MutationTaster2: mutation prediction for the deep-sequencing age. *Nat. Meth.*, **11**, 361–362.
56. Mathe, E., Olivier, M., Kato, S., Ishioka, C., Hainaut, P. and Tavtigian, S.V. (2006) Computational approaches for predicting the biological effect of p53 missense mutations: a comparison of three sequence analysis based methods. *Nucleic Acids Res.*, **34**, 1317–1325.
57. Tavtigian, S.V., Deffenbaugh, A.M., Yin, L., Judkins, T., Scholl, T., Samollow, P.B., de Silva, D., Zharkikh, A. and Thomas A. (2006) Comprehensive statistical study of 452 BRCA1 missense substitutions with classification of eight recurrent substitutions as neutral. *J. Med. Genet.*, **43**, 295–305.
58. Adzhubei, IA., Schmidt, S., Peshkin, L., Ramensky, VE., Gerasimova, A., Bork, P., Kondrashov AS. and Sunyaev, SR. (2010) A method and server for predicting damaging missense mutations. *Nat. Meth.*, **7**, 248–249.
59. Salgado, D., Desvignes JP., Rai, G., Blanchard, A., Miltgen, M., Pinard, A., Lévy, N., Collod-Béroud, G. and Béroud, C. (2016) UMD-Predictor: A high-throughput sequencing compliant system for pathogenicity prediction of any human cDNA substitution. *Hum. Mutat.*, **37**, 439–446.
60. Camargo, S.M.R., Singer, D., Makrides, V., Huggel, K., Pos, K.M., Wagner, C.A., Kuba, K., Danilczyk, U., Skovby, F., Kleta R., *et al.* (2009) Tissue-specific amino acid transporter partners ACE2 and collectrin differentially interact with hartnup mutations. *Gastroenterology*, **136**, 872–882.e3.